



ISSN: 0067-2904

Optimization of CuInSSe-Based Solar Cell Simulated by SCAPS-1D Software: Role of 30% Efficiency

Ameer F. Abdulameer*¹ Burak Yahya Kadem², R.K. Fakher Alfahed³, Mohammed K. Al Hashimi⁴

¹College of Science, University of Baghdad, Jadriya, Baghdad, Iraq

²College of Science, Al-Karkh University of Science, Baghdad, Iraq

³ Al-Nahrain Renewable Energy Research Center, Al-Nahrain University, Jadriya, Baghdad, Iraq

⁴College of Education, University of Misan, Misan, Iraq

Received: 1/12/2024

Accepted: 4/ 5/2025

Published: 30/3/2026

Abstract:

Copper Indium Sulfur-Selenide (CISSe)-based solar cell is examined by optimization several aspects including absorber layer thickness, buffer layer thickness, window layer thickness, working temperatures and energy band gap values. The optimization of these factors has resulted in optimum absorber layer thickness of 3000 nm, optimum CdS thickness of 10 nm, optimum ZnO thickness of 10 nm, optimum working temperature of 300 K and optimum energy band gap of 1.5 eV. The best device performance consisting of these optimum values results in a PCE of 30.51% correlated to FF of 83.7%, J_{SC} of 47.188 mA.cm⁻² and V_{OC} of 0.773 Volt. The results are promising and pave the way towards high PCE of CISSe-based solar. However, there might be a differences when these factors are applied in an experimental procedure due to the preparation conditions.

Keywords: SCAPS-1D; CISSe; Buffer layer; Thin film solar cell; CdS

خلية شمسية فعالة تعتمد على CuInSSe تمت محاكاتها بواسطة برنامج SCAPS-1D: دور الكفاءة بنسبة 30%

امير فيصل عبد الامير*¹, براق يحيى كاظم², رائد كاظم فاخر الفهد³, محمد كاظم الهاشمي⁴

¹كلية العلوم, جامعة بغداد, الجادرية, بغداد, العراق.

²كلية العلوم, جامعة الكرخ للعلوم, بغداد, العراق.

³مركز النهريين لبحوث الطاقة المتجددة, جامعة النهريين, الجادرية, بغداد, العراق.

⁴كلية التربية, جامعة ميسان, ميسان, العراق.

الخلاصة:

تم فحص الخلية الشمسية القائمة على سيلينييد النحاس والاندنيوم والكبريت (CISSe) من خلال تحسين مجموعة من الجوانب من ضمنها سمك طبقة الامتصاص, سمك طبقة العازل, وسمك الطبقة النافذة, درجة حرارة العمل و قيم فجوة الطاقة. افضل نتيجة لهذه العوامل كانت 300 نانو متر لامثل سمك لطبقة الامتصاص, سمك الاقراص المضغوطة عند 10 نانو متر, والسمك الامثل لأكسيد الخارصين 10 نانو متر, 300 كلفن كمثل درجة حرارة للعمل, فجوة الطاقة المثلى تكون 1.5 إلكترون - فولت. افضل اداء

* Email: ameer.abdulameer@sc.uobaghdad.edu.iq

للجهاز من هذه القيم المثلى ينتج عنه 30.51% من PCE المرتبط مع 83.7% من FF، 47.188 ملي امبير . سم² من J_{sc} و 0.773 فولت من V_{oc} . النتائج واعدة وتمهد الطريق نحو PCE عالية للطاقة الشمسية و القائمة على CISSe. ومع ذلك، قد تكون هناك اختلافات عند تطبيق هذه العوامل في إجراء تجريبي بسبب ظروف التحضير.

Introduction:

Among several important light-absorbing semiconductors used for thin film solar cells, I–III–VI group compounds are one of the promising absorber materials of Power Conversion Efficiency (PCE) higher than 20% at the laboratory scale and 15% at the module scale [1]. Copper Indium Sulfur-Selenide, abbreviated as (CISSe) has promising electrical and optical characteristics with a direct band gap ranging from 1eV to 1.5 eV depending on the S/Se ratio and an absorption coefficient higher than 10^5 cm^{-1} , making this material ideal for solar cell fabrication [2]. CISSe-based solar cells are categorized by their high PCE, low production cost, and stable performance [3]. To achieve high performance solar cell, several aspects should be considered, such as the absorber layer thickness [4], buffer layer [5], window layer [6], and working conditions [7]. One of the main issues that should be optimized to achieve high-performance solar cells is the buffer layer, as it directly affects the band alignment and interface between the absorber and the window layers [8]. Cadmium sulfide (CdS) is a favorable buffer layer used in thin film-based solar cells due to its 2.42 eV band gap, which contributes to a higher transmission in the blue wavelength region and enhances the interface with the absorber layer [9]. Ghebouli et al. [10] have examined a CISSe-based solar cell using a solar cell capacitance simulator (SCAPS-1D) software and estimated that the desired thickness of the CISSe absorber layer was 1800 nm. They achieved a PCE of 18.53 % using Zn_2SnO_4 buffer layer correlated with an open-circuit voltage (V_{oc}) of 0.5153 Volt, short-circuit current density (J_{sc}) of 45.4 mA.cm^{-2} and a fill factor (FF) of 79.17% compared to CdS buffer layer. They attributed the enhancement to the higher transmission properties of Zn_2SnO_4 layer due to its high band gap of 3.35 eV compared to 2.4 eV band gap of CdS. Furthermore, CISSe-based solar cell was examined using SCAPS-1D software employing In_2S_3 as the buffer layer, a PCE of 17.26% associated with a FF of 77.31%, J_{sc} of $45.0161 \text{ mA.cm}^{-2}$ and V_{oc} of 0.4958 Volt was achieved [11].

This study aims to achieve a 30% efficiency by controlling several parameters, including CISSe band gap and thickness, CdS thickness, and ZnO thickness. The simulated results and analysis through several steps and choosing the optimum parameters of each step are carried out. However, some parameters may differ between simulation and experimental studies due to several aspects, such as working conditions. However, the final output is promising to pave the way towards high performance CISSe solar cells.

Methodology and device structure:

SCAPS-1D version (3.3.07) is a one-dimensional solar cell simulation software developed at the Department of Electronics and Information Systems (EIS), University of Gent, Belgium, and was used for numerically analyzing the solar cell; all the details about the software were reported by Burgelman et al. [12]. The structure of the CISSe solar cell is composed of different layers, starting with the right contact, which is suggested to be a transparent conducting layer known as indium tin oxide (ITO), which is used to provide high light transparency and low sheet resistance [13]. In this work, the effect of series or shunt resistance was not considered; a similar consideration has been done by Jhuma et al. [14]. A ZnO layer was used as a window layer, followed by a buffer layer of a CdS layer; then a CISSe absorber layer was inserted, followed by the left Au contact with a work function of

5.146 eV as suggested by the software. SCAPS-1D software suggested a band gap value of 1.04 eV for the CISSe. The illumination was AMG1_5G_1sun with a power of 1000 W/m². The study was performed in several steps, first, optimizing the absorber layer thickness, which was varied from 500 nm to 3000 nm with equal steps of 100 nm and keeping other parameters, such as ZnO thickness of 200 nm, CdS thickness of 100nm, CISSe band gap of 1.04 eV, and working temperature at 300K, fixed. The second step was changing the buffer layer thickness from 10 nm to 100 nm with a step of 10 nm while keeping the absorber layer fixed at the optimum thickness. Following these steps, the optimum thicknesses of CISSe and CdS layers were used. The working temperature in the range of 300K to 350K with steps of 10K was evaluated, and the optimum working temperature was used. Moreover, the thickness of the ZnO layer was examined in the range from 10 nm to 200 nm with a 10 nm step and the optimum thickness was employed. Finally, the energy band varied from 1.04 eV to 1.5 eV, and the optimum band gap was chosen. The final optimum device with the optimum parameters was investigated. All the layers' characteristics used in this study are shown in Table 1.

Table 1: Material characteristics used in SCAPS -1D software to simulate the CISSe solar cell

Materials	ZnO	CdS	CISSe
Thickness (nm)	(10-200)	(10-100)	(500-3000)
Band gap (eV)	3.3	2.42	(1-1.5)
Electron affinity (eV)	4.1	4.1	4.3
Dielectric permittivity	9	9	12
CB effective density of state (1/cm ³)	4x10 ¹⁸	3 x10 ¹⁸	1 x10 ¹⁹
VB effective density of state (1/cm ³)	1 x10 ¹⁹	1.8 x10 ¹⁹	1 x10 ¹⁹
Electron thermal velocity (cm/s)	1 x10 ⁸	1 x10 ⁷	1 x10 ⁷
Hole on thermal velocity (cm/s)	1 x10 ⁸	1 x10 ⁷	1 x10 ⁷
Electron mobility (cm/Vs)	100	100	100
Electron mobility (cm/Vs)	20	25	25
Shallow donor density (1/cm ³)	1 x10 ¹⁸	1 x10 ¹⁷	1 x10 ⁵
Shallow acceptor density (1/cm ³)	1 x10 ⁵	1 x10 ⁵	1 x10 ¹⁶

The improvement in the device performance was mainly achieved when photogenerated carriers were extracted without experiencing recombination loss. The solar cell parameters were extracted based on the following equations [15]:

$$\text{PCE (\%)} = \frac{J_{\text{max}} V_{\text{max}}}{P_{\text{in}}} \quad (1)$$

$$\text{FF} = \frac{J_{\text{max}} V_{\text{max}}}{J_{\text{sc}} V_{\text{oc}}} \quad (2)$$

where P_{in} is the incident light power and J_{max} (mA.cm⁻²) and V_{max} (V) are the current density and voltage at the point of maximum power output in the J-V curves, respectively.

Results and discussions:

1. Controlling CISSe thickness:

The absorber layer CISSe thickness in a simulated CISSe-based solar cell was changed in the range from 500 nm to 3000 nm, with a ZnO layer thickness of 200 nm and that of CdS 100nm. An efficiency of 22.5% has resulted with an optimum CISSe thickness of 3000 nm [11]. In this study, changing the absorber layer thickness directly impacted the solar cell performance, as shown in Fig.1.

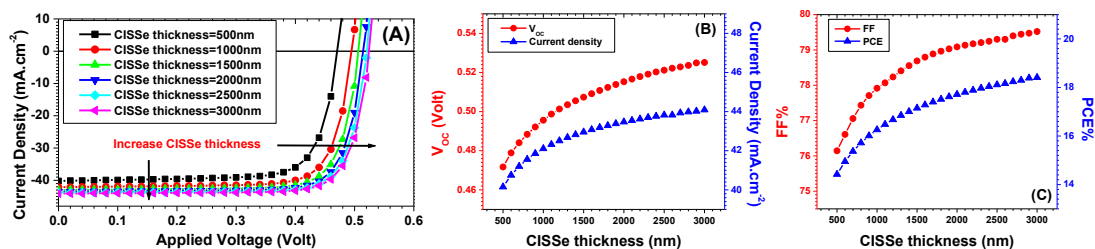


Figure 1: (A) Solar cell curves, (B) V_{oc} and J_{sc} and (C) FF and PCE, characteristics of the CISSe based solar cell with different CISSe thickness

Increasing the CISSe thickness resulted in increasing PCE from 14.4% for the 500 nm thickness to 18.41% for the 3000 nm thickness, FF from 76.14% to 79.52%, J_{SC} from 40.15 $\text{mA}\cdot\text{cm}^{-2}$ to 44.09 $\text{mA}\cdot\text{cm}^{-2}$, and V_{OC} from 0.472 Volt to 0.525 Volt. Such an increase is beneficial for higher solar cell performance and paves the way for experimental studies. However, the results might be altered when an experimental procedure is applied due to the preparation conditions. The increase in the solar cell performance may be attributed to different band energy alignments, as shown in Fig.2. When the thickness of the CISSe layer was 500 nm (Fig.2A), the band bending was different than that of 3000 nm thickness (Fig.2F).

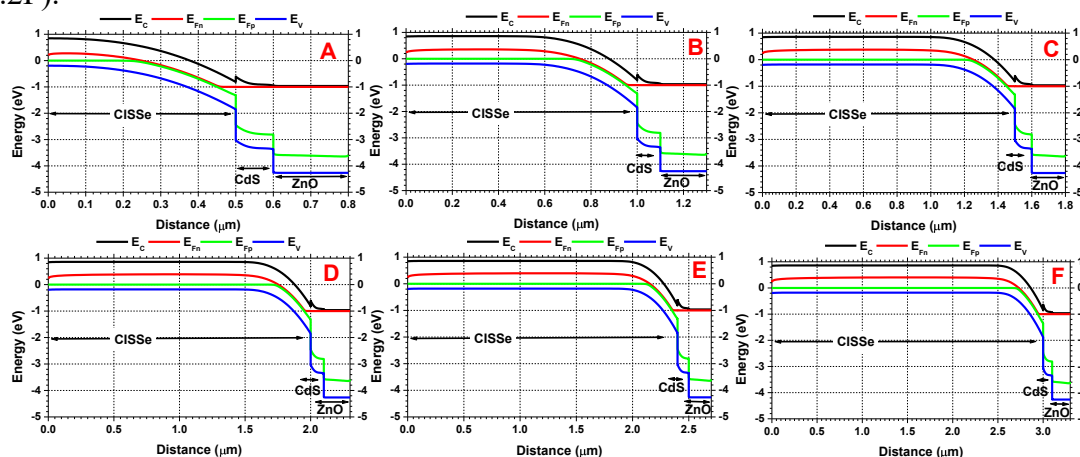


Figure 2: Energy band alignment of the CISSe based solar cell with different CISSe thickness (A) 0.5 μm , (B) 1 μm , (C) 1.5 μm , (D) 2 μm , (E) 2.5 μm and (F) 3 μm

The effect of absorber layer thickness variation was also studied by Ghebouli et al. [10], revealing that the optimal thickness for CISSe was 1800 nm. At this thickness, a PCE of 18.53%, a V_{OC} of 0.5153 V, a J_{SC} of 45.4 $\text{mA}\cdot\text{cm}^{-2}$, and an FF of 79.17% were achieved. They have attributed these results to the higher transmittance characteristics of the buffer layer in the short wavelength range. They also observed that J_{SC} , PCE, V_{OC} and FF increased with increasing CISSe thickness. This was attributed to the higher absorption properties of the thicker absorber layer, which produced more charge carriers.

The CISSe layer thickness variation has altered the Quasi-Fermi Levels (QFL), especially close to the CISSe\CdS interface and increased the internal voltage of the device [16]. A thicker CISSe layer is recommended to achieve higher solar cell performance. In this study, a thickness of 3000 nm was found to be the optimum thickness for better CISSe solar cell performance. Therefore, in the following sections, the thickness of the CISSe absorber layer was fixed at the optimum CISSe thickness.

2. Different working temperatures

SCAPS-1D software can propose the working temperature to evaluate the best working conditions for the prepared CISSe-based solar cells; in this context, different working temperatures in the range of (300K-350K) were performed to assess the solar cell performance. The solar cell structure of this section is [CISSe (3000 nm)/CdS (100 nm)/ZnO (200 nm)]. It is obvious from Fig.3 that increasing the working temperature results in performance reduction. Decreasing the temperature from 300K to 350K resulted in the decrease of: PCE from 18.41% to 13.79, FF from 79.52% to 74.03% and V_{OC} from 0.525 Volt to 0.421 Volt, while J_{SC} exhibited slight increase from 44.09 mA.cm⁻² to 44.2 mA.cm⁻².

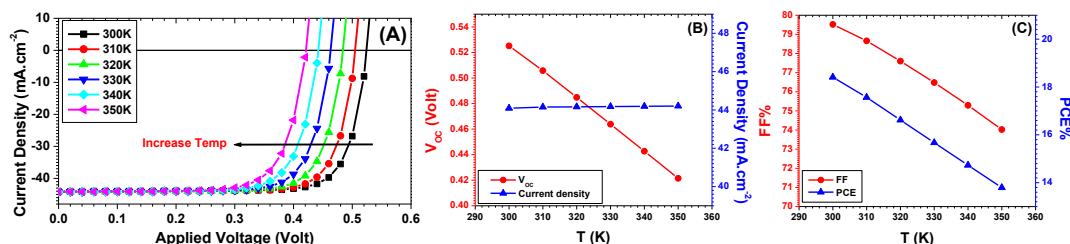


Figure 3: (A) Solar cell curves, (B) V_{oc} and J_{sc} and (C) FF and PCE, of the CISSe based solar cell at different working temperatures

Generally, increasing temperature results in linear decrease in V_{OC} [17], while J_{SC} increases slowly [18]. The variation in band structure between the devices treated at 300K and 350K is shown in Fig.4. The shifting of the electron Quasi Fermi Level (QFL) (E_{fn}) closer to the holes QFL (E_{fp}) reduces V_{OC} . Mainly V_{OC} is determined by the difference between E_{fn} and E_{fp} under open circuit condition using the following relation [19]:

$$V_{OC} = \frac{E_{fn} - E_{fp}}{q} \dots\dots\dots (3)$$

To achieve high solar cell performance, 300K was suggested as an optimum working temperature for CISSe-based solar cell with absorber layer thickness of 3000nm. Ghebouli et al. have also suggested that 300K is the best working temperature for CISSe-based solar cell [10].

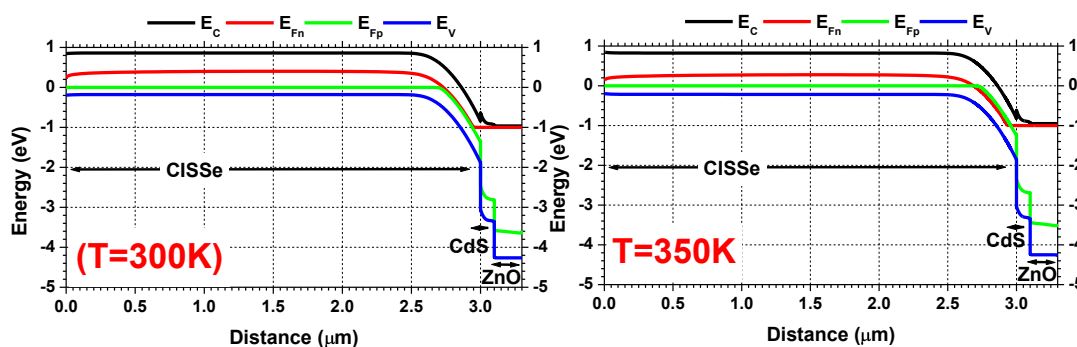


Figure 4: Energy band alignment of the CISSe-based solar cell at working temperatures (300K and 350K)

3. Different CdS layer thickness

The effects of the CdS buffer layer thickness ranging from 10 nm to 100 nm was investigated in this section. SCAPS-1D software suggests the use of 100 nm as a CdS thickness. However, variation is desired to achieve the optimum buffer layer thickness towards a 30% efficiency solar cell. Fig.5 illustrates the performance of the investigated CISSe-based solar cell with different CdS layer thicknesses; a thinner CdS layer resulted in

higher PCE of 19.75% associated with FF of 80.03%, J_{SC} of $46.16 \text{ mA}\cdot\text{cm}^{-2}$, and V_{OC} of 0.525 Volt. This increase in the device performance with decreasing the buffer layer thickness is attributed to the probability of reducing the recombination rate and thus increasing the current density and PCE [20]. Reducing the buffer layer thickness is beneficial for light absorption, as the light passes through the window layer (ZnO) to the buffer layer (CdS) and then to the absorber layer (CISSe); thinner thickness is better for higher transmittance characteristics and higher production of electron-hole pair [21].

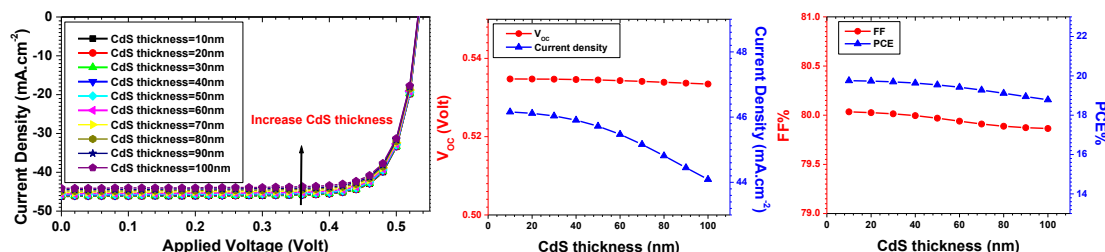


Figure 5: Solar cell parameters of the CISSe-based solar cell with different CdS layer thickness.

Moreover, FF decreases from 80.03% (when the CdS thickness was 10 nm) to 79.86% (for a CdS thickness of 100 nm) due to the increase in the series resistance with thickness and the maximum possible power output also decreased [22]. PCE for the different buffer layer thicknesses followed the FF trend. The reduction in PCE was attributed to the combined effect of J_{SC} and FF [14]. However, V_{OC} exhibited no apparent change as the QFL was not affected by the buffer layer thickness, as shown in Fig.6. Jhuma et al. [14] have examined the effect of CdS layer thickness in the range from 50 nm to 150 nm for a CZTS-based solar cell. They found that the buffer layer has no effect on the V_{OC} . In this study, the improvement of PCE of the CISSe-based solar cell using 10 nm thickness of CdS was encouraging to suggest that this is the optimum thickness.

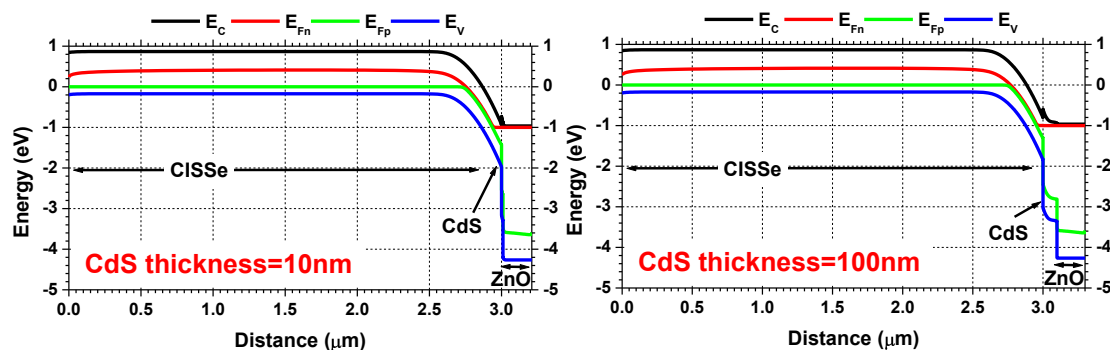


Figure 6: Energy band alignment of the CISSe based solar cell with 10nm and 100nm CdS layer thickness

4. Different band gap of CISSe

Usually, CISSe materials have a range of band gaps (E_g) from approximately 1.0 eV to 1.5 eV, which enables them to absorb a significant portion of the solar spectrum. This range of band gap of CISSe composition is attributed to various aspects, such as the ratio of copper, indium, sulfur, and selenium within the material [2,3]. For this reason, the optimization of the CISSe band gap was carried out, and a maximum of 30% efficiency was the main target. It is worth noting that the devices' performance has increased incredibly by changing the band gap value, as shown in Fig.7. PCE increased from 22.04% when a 1.1eV band gap was used,

whereas increasing the band gap to 1.5eV achieved as high a PCE as 29.88%. FF increased from 81.19% in the device with an E_g of 1.1eV to 83.66% in the device with an E_g of 1.5eV.

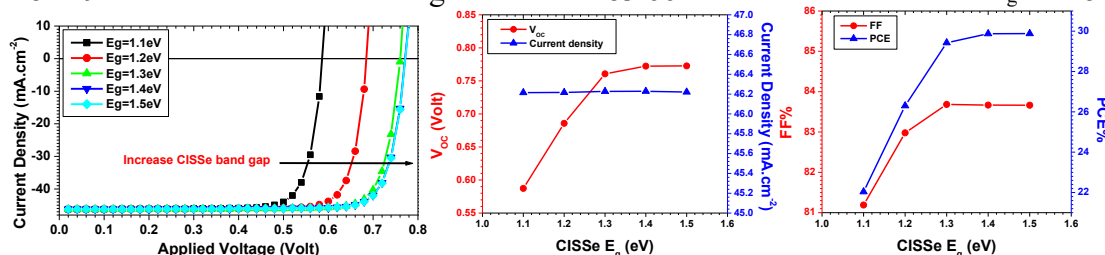


Figure 7: Solar cell parameters of the CISSe-based solar cell with different energy bands of CISSe.

Moreover, V_{OC} improved dramatically from 0.59 Volt when E_g was 1.1eV to 0.773V when E_g increased to 1.5eV; while J_{SC} showed no clear change in their values. Such variation in the device performance was attributed to the band gap increase from 1eV to 1.5eV, both E_{fn} and E_{fp} exhibited different positions closer to their respective conduction and valance bands, respectively, as shown in Fig.8. Such behavior is responsible for increasing the V_{OC} as it is mainly defined by these two factors [19]. The increase in the band gap and V_{OC} values directly affected the final output power. The optimization of the buffer layer resulting in increasing the FF was attributed to the good interface properties defined as low series resistance when 10 nm thickness of the CdS layer was used [22]. It was observed that FF decreased with increasing the buffer layer thickness due to the effect of series resistance and reduced the maximum achievable power output [14].

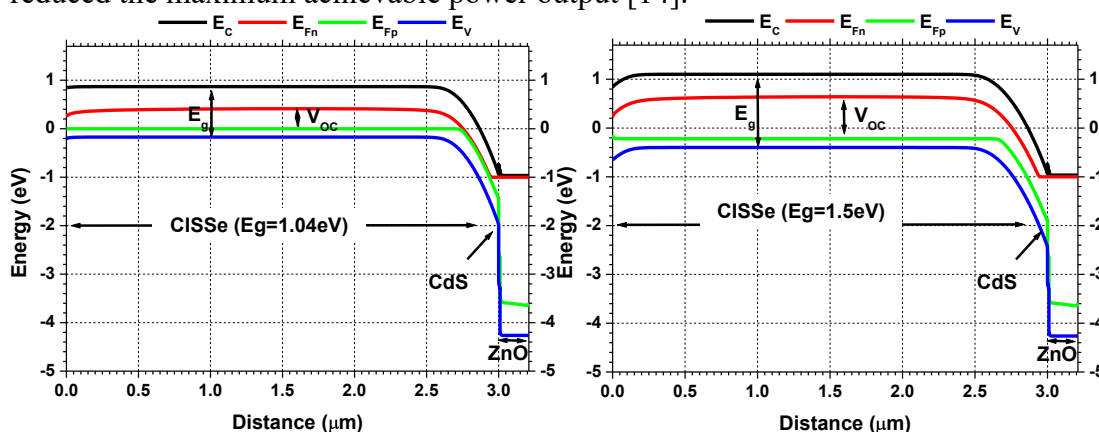


Figure 8: Energy band alignment of the CISSe based solar cell with different proposed band gaps of CISSe

For the above-mentioned reasons and the enhancement in the device performance, the band gap of 1.5eV was recommended as an optimum band gap for the CISSe material in CISSe-based solar cell. However, the preparation conditions could play a significant role in changing some of these results.

5. Different ZnO layer thickness

The window layer made of ZnO was also optimized by choosing different thicknesses ranging from 10 nm to 200 nm with an increase of 10 nm for each test. The results, in general, showed no big enhancement in the device performance compared to the previous section. However, achieving 30% was reached by this adjustment. FF and V_{OC} have demonstrated no change in their values; J_{SC} increased from 46.22 mA.cm⁻² in the device with a ZnO thickness of 200 nm to 47.188 mA.cm⁻² in the device with a 10 nm ZnO thickness. This increase was attributed to the increase in the absorption passing through the window

layer to the absorber layer, which increased the charge carrier generation inside the absorbing layer, resulting in more current density. The slight increase to reach a PCE as high as 30.51% in the device with a ZnO thickness of 10 nm was achieved, and this is mainly attributed to the increase in the current density [23].

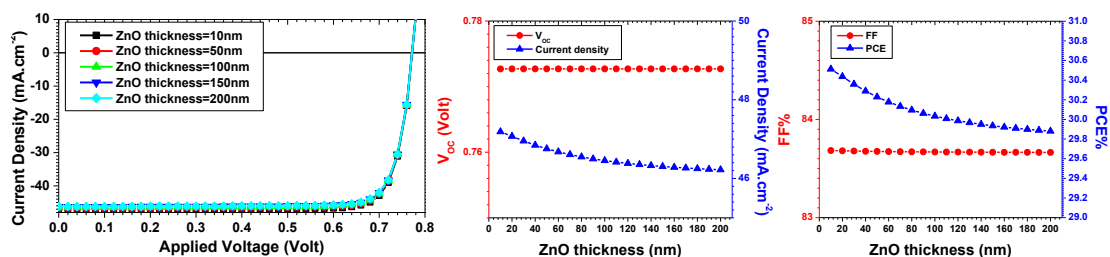


Figure 9: Solar cell parameters of the CISSe-based solar cell with different ZnO layer thicknesses

6. The optimum device performance

The optimum device performance in this study (see Fig.10) was achieved by controlling several factors as mentioned earlier as follows: ZnO (window layer) with 10 nm thickness, CdS (buffer layer) with 10 nm thickness, CISSe (absorber layer) with 3000 nm thickness, band gap of 1.5eV. This device achieved PCE of 30.5125% correlated with an FF of 0.83.7%, J_{sc} of 47.188 $\text{mA}\cdot\text{cm}^{-2}$, and V_{oc} of 0.773 Volt.

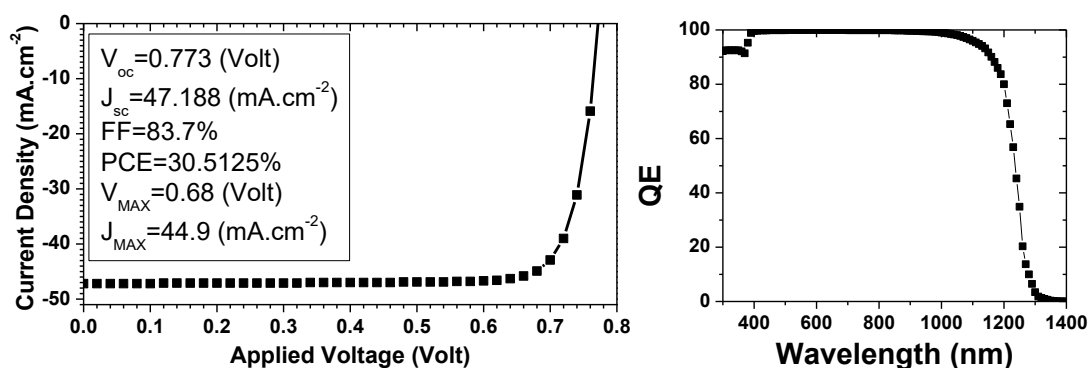


Figure 10: The best solar cell device achieved in this study based on the optimum parameters

The quantum efficiency (QE) of this device shown in Fig.10 demonstrates significant absorption region covering the wavelengths from around 300 nm to 1300 nm, which is very important for generating charge carriers and high performance solar cells. Zhang et al. reported closer results using CIS\CISSe graded band gap structure using SCAPS-1D software [24]. Ying et al. also reported similar results using wxAMPS software to simulate CuInSe_2 solar cells [25].

Conclusion:

This study aimed to achieve 30% efficiency in CISSe-based solar cells by optimizing key parameters, including the absorber, buffer, and window layers' thickness, the working temperature and the absorber layer band gap. Simulations using SCAPS-1D software indicated that the highest efficiency of 30.5125% was achieved with a CISSe absorber layer of 3000 nm and a band gap of 1.5 eV, a CdS buffer layer of 10 nm, and a ZnO window layer of 10 nm. The optimal working temperature was determined to be 300 K. The results demonstrated a high fill factor (FF) of 83.7%, a short-circuit current density (J_{sc}) of 47.188 $\text{mA}\cdot\text{cm}^{-2}$, and an open-circuit voltage (V_{oc}) of 0.773 V. The optimization of the layers'

thickness contributed to enhancing current density, while the band gap directly influenced the increase in open-circuit voltage. These findings present promising potential for experimental validation, though variations may arise due to differences in fabrication conditions.

Acknowledgment:

The author would like to acknowledge Dr. Hana Zerfaoui from Algeria, for her assistance in some simulation procedure steps.

References:

- [1] S. Lugo, Y. Sánchez, M. Neuschitzer, H. Xie, C. Insignares-Cuello, V. Izquierdo-Roca, Y. Pena, and E. Saucedo, "Chemical bath deposition route for the synthesis of ultra-thin $\text{CuIn}(\text{S},\text{Se})_2$ based solar cells," *Thin Solid Films*, vol. 582, pp. 74–78, 2015.
- [2] H. Liu, Z. Jin, J. Wang, J. Ao, and G. Li, "Well-dispersed CuInSe_2 nanoplates and nanoplates-ink-coated thin films for photovoltaic application by a triethylene glycol based solution process," *Materials Letters*, vol. 94, pp. 1–4, 2013.
- [3] F. Zhang, Q. Yu, H. W. Zhao, and Y. Zhao, "The numerical simulation of CIS/CISSe graded band gap solar cell using SCAPS-1D software," *Journal of Nanoparticle Research*, vol. 25, no. 12, p. 256, 2023.
- [4] T. Ouslimane, L. Et-Taya, L. Elmaimouni, and A. Benami, "Impact of absorber layer thickness, defect density, and operating temperature on the performance of MAPbI_3 solar cells based on ZnO electron transporting material," *Heliyon*, vol. 7, no. 3, p. e06379, 2021.
- [5] A. E. H. Benzetta, A. M. Mahfoud, and D. M. Elamine, "Numerical analysis of potential buffer layer for $\text{Cu}_2\text{ZnSnS}_4$ (CZTS) solar cells," *Optik*, vol. 204, p. 164155, 2020.
- [6] A. Bouarissa, A. Gueddim, N. Bouarissa, and H. Maghraoui-Meherezi, "Modeling of ZnO/MoS₂/CZTS photovoltaic solar cell through window, buffer and absorber layers optimization," *Materials Science and Engineering: B*, vol. 263, p. 114816, 2021.
- [7] A. D. Dhass, Y. Prakash, and K. C. Ramya, "Effect of temperature on internal parameters of solar cell," *Materials Today: Proceedings*, vol. 33, pp. 732–735, 2020.
- [8] W. Eisele, A. Ennaoui, P. Schubert-Bischoff, M. Giersig, C. Pettenkofer, J. Krauser, M. Lux-Steiner, S. Zweigart, and F. Karg, "XPS, TEM and NRA investigations of $\text{Zn}(\text{Se}, \text{OH})/\text{Zn}(\text{OH})_2$ films on $\text{Cu}(\text{In}, \text{Ga})(\text{S}, \text{Se})_2$ substrates for highly efficient solar cells," *Solar Energy Materials and Solar Cells*, vol. 75, no. 1–2, pp. 17–26, 2003.
- [9] M. Nguyen, K. Ernits, K. F. Tai, C. F. Ng, S. S. Pramana, W. A. Sasangka, S. K. Batabyal, T. Holopainen, D. Meissner, A. Neisser, and L. H. Wong, "ZnS buffer layer for $\text{Cu}_2\text{ZnSn}(\text{SSe})_4$ monograin layer solar cell," *Solar Energy*, vol. 111, pp. 344–349, 2015.
- [10] M. A. Ghebouli, B. Ghebouli, R. Larbi, T. Chihi, and M. Fatmi, "Effect of buffer nature, absorber layer thickness and temperature on the performance of CISSe based solar cells, using SCAPS-1D simulation program," *Optik*, vol. 241, p. 166203, 2021.
- [11] M. A. Ashraf and I. Alam, "Numerical simulation of CIGS, CISSe and CZTS-based solar cells with In_2S_3 as buffer layer and Au as back contact using SCAPS 1D," *Engineering Research Express*, vol. 2, no. 3, p. 035015, 2020.
- [12] M. Burgelman, K. Decock, A. Niemegeers, J. Verschraegen, and S. Degrave, *SCAPS manual*. Ghent, Belgium: University of Ghent, 2016.
- [13] T. J. Coutts, T. O. Mason, J. D. Perkins, and D. S. Ginley, "Transparent conducting oxides: status and opportunities in basic research," *Proceedings of the Electrochemical Society*, vol. 99, pp. 274–288, 1999.
- [14] F. A. Jhuma, M. Z. Shaily, and M. J. Rashid, "Towards high-efficiency CZTS solar cell through buffer layer optimization," *Materials for Renewable and Sustainable Energy*, vol. 8, pp. 1–7, 2019.
- [15] B. Y. Kadem, A. K. Hassan, and W. Cranton, "Enhancement of power conversion efficiency of P3HT:PCBM solar cell using solution processed Alq_3 film as electron transport layer," *Journal of Materials Science: Materials in Electronics*, vol. 26, pp. 3976–3983, 2015.
- [16] F. Babbe, L. Choubrac, and S. Siebentritt, "The optical diode ideality factor enables fast screening of semiconductors for solar cells," *Solar RRL*, vol. 2, no. 12, p. 1800248, 2018.

- [17] W. Bagiński, G. S. Kinsey, M. Liu, A. Nayak, V. Garboushian, F. Dimroth, F. Rubio, and I. Antón, "Open circuit voltage temperature coefficients vs. concentration: Theory, indoor measurements, and outdoor measurements," *AIP Conference Proceedings*, vol. 1477, no. 1, p. 148, 2012.
- [18] S. Azimi-Nam and F. Farhani, "Effect of temperature on electrical parameters of phosphorus spin-on diffusion of polysilicon solar cells," *Journal of Renewable Energy and Environment*, vol. 4, no. 1, pp. 41–45, 2017.
- [19] B. Y. Kadem, M. Al-Hashimi, A. S. Hasan, R. G. Kadhim, Y. Rahaq, and A. K. Hassan, "The effects of the PEDOT:PSS acidity on the performance and stability of P3HT:PCBM-based OSCs," *Journal of Materials Science: Materials in Electronics*, vol.29, pp. 19287–19295, 2018.
- [20] N. Benaya, A. Zoukel, M. M. Taouti, and M. Silaa, "The impact of the buffer layer material and active layer thickness on the performance of a fullerene-free organic solar cell," *International Conference on Applied Engineering and Natural Sciences*, vol. 1, no. 1, pp.338-341, 2023.
- [21] P. Lin, L. Lin, J. Yu, S. Cheng, P. Lu, and Q. Zheng, "Numerical simulation of $\text{Cu}_2\text{ZnSnS}_4$ based solar cells with In_2S_3 buffer layers by SCAPS-1D," *Journal of Applied Science and Engineering*, vol. 17, no. 4, pp. 383–390, 2014.
- [22] M. Dadu, A. Kapoor, and K. N. Tripathi, "Effect of operating current dependent series resistance on the fill factor of a solar cell," *Solar Energy Materials and Solar Cells*, vol. 71, no. 2, pp. 213–218, 2002.
- [23] E. Cho, J. G. Son, C. B. Park, I. Kim, D. Yuk, J. S. Park, J. Y. Kim, and S. J. Lee, "Highly improved photocurrent density and efficiency of perovskite solar cells via inclined fluorine sputtering process," *Advanced Functional Materials*, vol. 33, no. 25, p. 2301033, 2023.
- [24] F. Zhang, Q. Yu, H. W. Zhao, and Y. Zhao, "The numerical simulation of CIS/CISse graded band gap solar cell using SCAPS-1D software," *Journal of Nanoparticle Research*, vol. 25, no. 1, p. 256, 2023.
- [25] M. Ying, J. Wen, and Y. Zhao, "Numerical simulation of CuInSe_2 solar cells using wxAMPS software," *Chinese Journal of Physics*, vol. 76, pp. 24–34, 2002.